

Measurement of Branching Fractions and Polarization in $B \rightarrow \phi K^{(*)}$ Decays

K.-F. Chen,²³ A. Bozek,²⁴ K. Abe,⁷ K. Abe,³⁸ T. Abe,⁷ I. Adachi,⁷ H. Aihara,⁴⁰
M. Akatsu,¹⁹ Y. Asano,⁴⁵ T. Aso,⁴⁴ A. M. Bakich,³⁶ Y. Ban,³⁰ E. Banas,²⁴ A. Bay,¹⁵
P. K. Behera,⁴⁶ I. Bizjak,¹¹ A. Bondar,¹ M. Bračko,^{17,11} J. Brodzicka,²⁴ T. E. Browder,⁶
B. C. K. Casey,⁶ M.-C. Chang,²³ P. Chang,²³ Y. Chao,²³ B. G. Cheon,³⁵ R. Chistov,¹⁰
S.-K. Choi,⁵ Y. Choi,³⁵ Y. K. Choi,³⁵ M. Danilov,¹⁰ M. Dash,⁴⁷ L. Y. Dong,⁸
A. Drutskoy,¹⁰ S. Eidelman,¹ V. Eiges,¹⁰ Y. Enari,¹⁹ C. Fukunaga,⁴² N. Gabyshev,⁷
A. Garmash,^{1,7} T. Gershon,⁷ B. Golob,^{16,11} R. Guo,²¹ J. Haba,⁷ C. Hagner,⁴⁷ F. Handa,³⁹
H. Hayashii,²⁰ M. Hazumi,⁷ T. Higuchi,⁷ L. Hinz,¹⁵ T. Hokuue,¹⁹ Y. Hoshi,³⁸ W.-S. Hou,²³
Y. B. Hsiung,^{23,*} H.-C. Huang,²³ Y. Igarashi,⁷ T. Iijima,¹⁹ K. Inami,¹⁹ A. Ishikawa,¹⁹
H. Ishino,⁴¹ R. Itoh,⁷ H. Iwasaki,⁷ Y. Iwasaki,⁷ H. K. Jang,³⁴ M. Jones,⁶ J. H. Kang,⁴⁹
J. S. Kang,¹³ N. Katayama,⁷ H. Kawai,² H. Kawai,⁴⁰ T. Kawasaki,²⁶ H. Kichimi,⁷
D. W. Kim,³⁵ Hyunwoo Kim,¹³ J. H. Kim,³⁵ S. K. Kim,³⁴ K. Kinoshita,³ P. Koppenburg,⁷
S. Korpar,^{17,11} P. Krokovny,¹ A. Kuzmin,¹ Y.-J. Kwon,⁴⁹ J. S. Lange,^{4,32} S. H. Lee,³⁴
T. Lesiak,²⁴ J. Li,³³ A. Limosani,¹⁸ S.-W. Lin,²³ J. MacNaughton,⁹ F. Mandl,⁹
D. Marlow,³¹ H. Matsumoto,²⁶ T. Matsumoto,⁴² A. Matyja,²⁴ W. Mitaroff,⁹ H. Miyake,²⁸
H. Miyata,²⁶ D. Mohapatra,⁴⁷ T. Mori,⁴¹ T. Nagamine,³⁹ T. Nakadaira,⁴⁰ E. Nakano,²⁷
M. Nakao,⁷ J. W. Nam,³⁵ Z. Natkaniec,²⁴ S. Nishida,⁷ O. Nitoh,⁴³ T. Nozaki,⁷
S. Ogawa,³⁷ T. Ohshima,¹⁹ T. Okabe,¹⁹ S. Okuno,¹² S. L. Olsen,⁶ W. Ostrowicz,²⁴
H. Ozaki,⁷ H. Palka,²⁴ C. W. Park,¹³ H. Park,¹⁴ K. S. Park,³⁵ N. Parslow,³⁶ L. S. Peak,³⁶
M. Peters,⁶ L. E. Piilonen,⁴⁷ N. Root,¹ M. Rozanska,²⁴ H. Sagawa,⁷ S. Saitoh,⁷ Y. Sakai,⁷
T. R. Sarangi,⁴⁶ M. Satapathy,⁴⁶ A. Satpathy,^{7,3} O. Schneider,¹⁵ J. Schümamm,²³
A. J. Schwartz,³ S. Semenov,¹⁰ K. Senyo,¹⁹ M. E. Sevier,¹⁸ V. Sidorov,¹ J. B. Singh,²⁹
S. Stanič,^{45,†} M. Starič,¹¹ A. Sugi,¹⁹ K. Sumisawa,⁷ T. Sumiyoshi,⁴² S. Suzuki,⁴⁸
T. Takahashi,²⁷ F. Takasaki,⁷ K. Tamai,⁷ N. Tamura,²⁶ M. Tanaka,⁷ Y. Teramoto,²⁷
T. Tomura,⁴⁰ T. Tsuboyama,⁷ T. Tsukamoto,⁷ K. Ueno,²³ Y. Unno,² S. Uno,⁷ Y. Ushiroda,⁷
G. Varner,⁶ K. E. Varvell,³⁶ C. C. Wang,²³ C. H. Wang,²² J. G. Wang,⁴⁷ M.-Z. Wang,²³
M. Watanabe,²⁶ Y. Watanabe,⁴¹ E. Won,¹³ B. D. Yabsley,⁴⁷ Y. Yamada,⁷ A. Yamaguchi,³⁹
Y. Yamashita,²⁵ M. Yamauchi,⁷ H. Yanai,²⁶ P. Yeh,²³ M. Yokoyama,⁴⁰ Y. Yusa,³⁹
C. C. Zhang,⁸ J. Zhang,⁴⁵ Z. P. Zhang,³³ Y. Zheng,⁶ V. Zhilich,¹ and D. Žontar^{16,11}

(The Belle Collaboration)

¹*Budker Institute of Nuclear Physics, Novosibirsk*

²*Chiba University, Chiba*

³*University of Cincinnati, Cincinnati, Ohio 45221*

⁴*University of Frankfurt, Frankfurt*

⁵*Gyeongsang National University, Chinju*

⁶*University of Hawaii, Honolulu, Hawaii 96822*

⁷*High Energy Accelerator Research Organization (KEK), Tsukuba*

⁸*Institute of High Energy Physics, Chinese Academy of Sciences, Beijing*

⁹*Institute of High Energy Physics, Vienna*

¹⁰*Institute for Theoretical and Experimental Physics, Moscow*

¹¹*J. Stefan Institute, Ljubljana*

- ¹²*Kanagawa University, Yokohama*
¹³*Korea University, Seoul*
¹⁴*Kyungpook National University, Taegu*
¹⁵*Institut de Physique des Hautes Énergies, Université de Lausanne, Lausanne*
¹⁶*University of Ljubljana, Ljubljana*
¹⁷*University of Maribor, Maribor*
¹⁸*University of Melbourne, Victoria*
¹⁹*Nagoya University, Nagoya*
²⁰*Nara Women's University, Nara*
²¹*National Kaohsiung Normal University, Kaohsiung*
²²*National Lien-Ho Institute of Technology, Miao Li*
²³*Department of Physics, National Taiwan University, Taipei*
²⁴*H. Niewodniczanski Institute of Nuclear Physics, Krakow*
²⁵*Nihon Dental College, Niigata*
²⁶*Niigata University, Niigata*
²⁷*Osaka City University, Osaka*
²⁸*Osaka University, Osaka*
²⁹*Panjab University, Chandigarh*
³⁰*Peking University, Beijing*
³¹*Princeton University, Princeton, New Jersey 08545*
³²*RIKEN BNL Research Center, Upton, New York 11973*
³³*University of Science and Technology of China, Hefei*
³⁴*Seoul National University, Seoul*
³⁵*Sungkyunkwan University, Suwon*
³⁶*University of Sydney, Sydney NSW*
³⁷*Toho University, Funabashi*
³⁸*Tohoku Gakuin University, Tagajo*
³⁹*Tohoku University, Sendai*
⁴⁰*Department of Physics, University of Tokyo, Tokyo*
⁴¹*Tokyo Institute of Technology, Tokyo*
⁴²*Tokyo Metropolitan University, Tokyo*
⁴³*Tokyo University of Agriculture and Technology, Tokyo*
⁴⁴*Toyama National College of Maritime Technology, Toyama*
⁴⁵*University of Tsukuba, Tsukuba*
⁴⁶*Utkal University, Bhubaneswer*
⁴⁷*Virginia Polytechnic Institute and State University, Blacksburg, Virginia 24061*
⁴⁸*Yokkaichi University, Yokkaichi*
⁴⁹*Yonsei University, Seoul*

Abstract

We present the first measurement of decay amplitudes in $B \rightarrow \phi K^{*}$ and measurements of branching fractions in $B \rightarrow \phi K^{(*)}$ decays based on 78.1 fb^{-1} of data recorded at the $\Upsilon(4S)$ resonance with the Belle detector at the KEKB e^+e^- storage ring. The decay amplitudes for the different ϕK^{*0} helicity states are measured from the angular distributions of final state particles in the transversity basis. The longitudinal and transverse complex amplitudes are $|A_0|^2 = 0.43 \pm 0.09 \pm 0.04$, $|A_\perp|^2 = 0.41 \pm 0.10 \pm 0.04$, $\arg(A_\parallel) = -2.57 \pm 0.39 \pm 0.09$, and $\arg(A_\perp) = 0.48 \pm 0.32 \pm 0.06$. The direct CP -violating asymmetries are found to be consistent with zero.

PACS numbers: 13.25.Hw, 14.40.Nd

B meson decays involving $b \rightarrow s\bar{s}s$ transitions, such as $B \rightarrow \phi K$ and ϕK^* , are forbidden to first order in the Standard Model (SM), but proceed by second order loop diagrams (penguin and box diagrams), which lead to the flavor changing neutral current transition $b \rightarrow s$. These processes provide information on the Cabibbo-Kobayashi-Maskawa matrix element V_{ts} [1] and are sensitive to physics beyond the SM such as R-parity violating SUSY contributions to $b \rightarrow s\bar{s}s$ [2]. They can also be used to perform independent measurements of the CP -violating parameter $\sin 2\phi_1$ [3]. The branching fractions of $B \rightarrow \phi K$ have been predicted by QCD-factorization [4] and PQCD [5]. The decay $B \rightarrow \phi K^*$ is a mixture of CP -even and CP -odd states; polarization measurements allow us to project out the different CP states statistically.

In this letter, we report the first measurement of the helicity state amplitudes in $B^0 \rightarrow \phi K^{*0}$ decay by a full three-dimensional angular analysis. We also report measurements of branching fractions and direct CP asymmetries in $B^+ \rightarrow \phi K^+$, $B^0 \rightarrow \phi K^0$, $B^+ \rightarrow \phi K^{*+}$, and $B^0 \rightarrow \phi K^{*0}$ decays (charge conjugate modes are included everywhere unless otherwise specified).

This analysis is based on a data set with an integrated luminosity of 78.1 fb^{-1} taken at the $\Upsilon(4S)$ resonance recorded by the Belle detector [6] at the KEKB e^+e^- collider [7]. This luminosity corresponds to $(85.5 \pm 0.5) \times 10^6$ produced $B\bar{B}$ pairs. The beam energies are 8 GeV for e^- and 3.5 GeV for e^+ .

The Belle detector is a general purpose magnetic spectrometer equipped with a 1.5 T superconducting solenoid magnet. Charged tracks are reconstructed in a Central Drift Chamber (CDC) and a Silicon Vertex Detector (SVD). Photons and electrons are identified using a CsI(Tl) Electromagnetic Calorimeter (ECL) located inside the magnet coil. Charged particles are identified using measured dE/dx in the CDC as well as information from Aerogel Cherenkov Counters (ACC) and Time of Flight Counters (TOF). A kaon likelihood ratio, $P(K/\pi) = \mathcal{L}_K / (\mathcal{L}_K + \mathcal{L}_\pi)$, has values between 0 (likely to be a pion) and 1 (likely to be a kaon), where $\mathcal{L}_{K(\pi)}$ is derived from dE/dx , ACC and TOF measurements.

Candidate $\phi \rightarrow K^+K^-$ decays are found by selecting pairs of oppositely charged tracks that are not pion-like ($P(K/\pi) > 0.1$). The vertex of the candidate charged tracks is required to be consistent with the interaction point (IP) to suppress poorly measured tracks. In addition, candidates are required to have a K^+K^- invariant mass that is less than $10 \text{ MeV}/c^2$ from the nominal ϕ meson mass.

Pairs of oppositely charged tracks are used to reconstruct $K_S^0 \rightarrow \pi^+\pi^-$ decays. The $\pi^+\pi^-$ vertex is required to be displaced from the IP by a minimum transverse distance of 0.22 cm for high momentum ($> 1.5 \text{ GeV}/c$) candidates and 0.08 cm for those with momentum less than $1.5 \text{ GeV}/c$. The direction of the pion pair momentum must agree with the direction defined by the IP and the vertex displacement within 0.03 rad for high-momentum candidates, and within 0.1 rad for the remaining candidates.

Charged tracks with $P(K/\pi) > 0.4$ (< 0.9) are considered to be kaons (pions). For $\pi^0 \rightarrow \gamma\gamma$, a minimum photon energy of 50 MeV is required and the $\gamma\gamma$ invariant mass must be less than $16 \text{ MeV}/c^2$ from the nominal π^0 mass. K^* candidates are reconstructed in three decay modes: $K^{*0} \rightarrow K^+\pi^-$, $K^{*+} \rightarrow K^+\pi^0$ and $K^{*+} \rightarrow K_S^0\pi^+$. The invariant mass of the K^* candidate is required to be less than $70 \text{ MeV}/c^2$ from the nominal K^* mass.

A B meson is reconstructed from a ϕ meson candidate and a K or K^* candidate and identified by the energy difference $\Delta E \equiv E_B^{\text{cms}} - E_{\text{beam}}^{\text{cms}}$, and the beam constrained mass $M_{\text{bc}} \equiv \sqrt{(E_{\text{beam}}^{\text{cms}})^2 - (p_B^{\text{cms}})^2}$. $E_{\text{beam}}^{\text{cms}}$ is the beam energy in the center-of-mass system (cms) of the $\Upsilon(4S)$ resonance, and E_B^{cms} and p_B^{cms} are the cms energy and momentum of the

reconstructed B candidate. The B -meson signal window is defined as $5.27 \text{ GeV}/c^2 < M_{bc} < 5.29 \text{ GeV}/c^2$ and $|\Delta E| < 64$ (60) MeV for $B \rightarrow \phi K$ ($B \rightarrow \phi K^*$). The signal window is enlarged to $-100 \text{ MeV} < \Delta E < 80 \text{ MeV}$ for $B^+ \rightarrow \phi K^{*+}$ ($K^{*+} \rightarrow K^+ \pi^0$) because of the impact of shower leakage on ΔE resolution. An additional requirement $\cos \theta_{K^*} < 0.8$ is applied to reduce low momentum π^0 background, where θ_{K^*} is the angle between the K^* direction and its daughter kaon defined in the K^* rest frame. In the signal window about 1% of the events have multiple candidates. We choose the best candidate according to the value of the B vertex χ^2 .

The dominant background is continuum $e^+e^- \rightarrow q\bar{q}$ production ($q = u, d, c, s$). Several variables are used to exploit the differences between the event shapes for continuum $q\bar{q}$ production (jet-like) and for B decay (spherical) in the cms frame of the $\Upsilon(4S)$ [8]. These variables are combined into a single likelihood ratio $R_s = \mathcal{L}_s/(\mathcal{L}_s + \mathcal{L}_{q\bar{q}})$, where \mathcal{L}_s ($\mathcal{L}_{q\bar{q}}$) denotes the signal (continuum) likelihood. An additional variable $\cos \theta_H$, which is the angle between the ϕ momentum and the daughter kaon momentum in the ϕ rest frame, is included for the ϕK^+ and ϕK_S^0 channels.

Backgrounds from other B decay modes such as $B \rightarrow KKK^{(*)}$, $B \rightarrow f_0(980)K^{(*)}$ ($f_0 \rightarrow K^+K^-$), $B \rightarrow \phi K\pi$, $B \rightarrow KKK\pi$, and feed-across between ϕK^* and ϕK decay channels are studied. The contributions from $B \rightarrow KKK^{(*)}$ and $B \rightarrow f_0(980)K^{(*)}$ ($f_0 \rightarrow K^+K^-$) are estimated from the K^+K^- invariant mass distribution. The K^+K^- mass distribution for $B \rightarrow KKK^{(*)}$ is determined by Monte Carlo (MC) simulation assuming three-body phase space decay. The shape for $f_0(980)$ is obtained from MC, where a Breit-Wigner with a 40 MeV/ c^2 intrinsic width is assumed. These contributions are estimated separately by fits to the events outside of the ϕ mass region. The contribution from $B \rightarrow KKK^{(*)}$ is estimated to be 5–9% [9] of the signal yield and is subtracted from the raw signal yield. The $B \rightarrow f_0K^{(*)}$ contribution is estimated to be 2–12%. The large uncertainty in the intrinsic width of the $f_0(980)$ is included in the systematic error. The background from $B \rightarrow \phi K\pi$ decay, as well as higher K^* resonance decay, is studied by performing fits to the $K\pi$ invariant mass. The estimated background (1–3%) is considered as a systematic error. Contamination from four-body $B \rightarrow KKKK\pi$ decays is checked by performing fits to the non-resonant region of K^+K^- and $K\pi$ mass. It is found to be very small and is neglected. The feed-across from ϕK^* in ϕK decay is removed by excluding events with $\Delta E < -120$ MeV from the fit. A veto is applied in $B \rightarrow \phi K^*$ channels to remove the feed-across background from ϕK .

The signal yields (N_s) are extracted by extended unbinned maximum-likelihood fits performed in ΔE and M_{bc} simultaneously. The signal probability density functions (PDFs) are represented by Gaussians for both ΔE and M_{bc} . The means and widths are verified using $B^+ \rightarrow \bar{D}^0\pi^+$ and $B \rightarrow J/\psi K^*$ decays. Additional bifurcated Gaussians (Gaussians with different widths on either side of the mean) are used to model the tails in the ΔE distribution of ϕK^* channels. The continuum PDF for M_{bc} (ΔE) is determined from the events outside of ΔE (M_{bc}) signal window. The continuum PDFs for M_{bc} and ΔE are represented by an empirical background function introduced by ARGUS [10] and a linear function, respectively. The number of signal and background are floated in the fit while other PDF parameters are fixed. The measured branching fractions (\mathcal{B}) are summarized in Table I. The distributions of ΔE and M_{bc} for the four measured modes are shown in Fig. 1.

The systematic errors in the signal yields are estimated by varying each fixed PDF parameter by $\pm 1\sigma$ of its nominal value. Conservatively, the change in the signal yield from each variation is added in quadrature. The systematic errors in the efficiency are due to uncertainties in track finding (1% per track), particle identification (2%), K_S^0 and π^0 finding

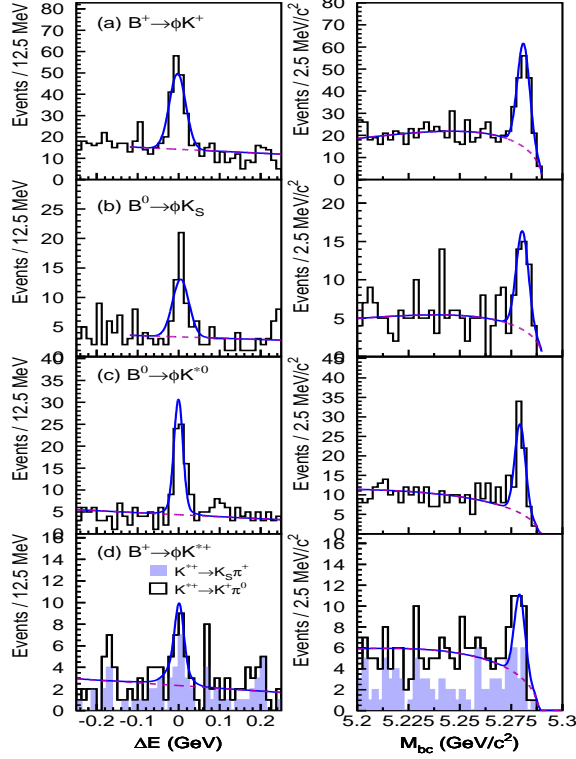


FIG. 1: Distributions of ΔE (M_{bc}) with fit results for the events in the M_{bc} (ΔE) signal window. The continuum background component is shown by dashed curves.

TABLE I: Signal yields (N_s) obtained by fits after background subtraction, total efficiency (ϵ), statistical significance ($\Sigma \equiv \sqrt{2 \ln[\mathcal{L}(N_s)/\mathcal{L}(0)]}$), and measured branching fraction (\mathcal{B}). The intermediate branching fractions are taken from [11].

Mode	N_s	ϵ (%)	Σ	$\mathcal{B}(10^{-6})$
$B^+ \rightarrow \phi K^+$	136^{+16}_{-15}	16.9	16.5	$9.4 \pm 1.1 \pm 0.7$
$B^0 \rightarrow \phi K^0$	$35.6^{+8.4}_{-7.4}$	4.6	8.7	$9.0^{+2.2}_{-1.8} \pm 0.7$
$B^0 \rightarrow \phi K^{*0}$	$58.5^{+9.1}_{-8.1}$	6.9	11.3	$10.0^{+1.6}_{-1.5} \pm 0.7$
$B^+ \rightarrow \phi K^{*+}$	—	—	4.9	$6.7^{+2.1}_{-1.9} \pm 0.7$
$K^{*+} \rightarrow K^+ \pi^0$	$8.0^{+4.3}_{-3.5}$	1.4	2.8	$6.9^{+3.8}_{-3.2} \pm 0.9$
$K^{*+} \rightarrow K_S^0 \pi^+$	$11.3^{+4.5}_{-3.8}$	2.1	4.0	$6.5^{+2.6}_{-2.3} \pm 0.6$

(4%), and to the uncertainty in $\mathcal{B}(\phi \rightarrow K^+ K^-)$ (1.4%). The estimated contaminations of $B \rightarrow f_0 K^{(*)}$ and $B \rightarrow \phi K \pi$ are included as an uncertainty in the background. For the $B \rightarrow \phi K^*$ modes, an additional systematic error in the efficiency due to the uncertainty in the polarization together with the uncertainty in the slow pion detection efficiency (1%-4%) is included.

For the self-tagging modes $B^+ \rightarrow \phi K^+$, $B^0 \rightarrow \phi K^{*0}(K^+ \pi^-)$, and $B^+ \rightarrow \phi K^{*+}$ we have studied the direct CP asymmetries $A_{CP} = \frac{N(\overline{B} \rightarrow \overline{f}) - N(B \rightarrow f)}{N(\overline{B} \rightarrow \overline{f}) + N(B \rightarrow f)}$, where B (\overline{B}) is B^0 or B^+ (B^0 or B^-) and f is one of the self-tagged $\phi K^{(*)}$ final states. The values of A_{CP} for $B^+ \rightarrow$

ϕK^+ , $B^0 \rightarrow \phi K^{*0}(K^+\pi^-)$, and $B^+ \rightarrow \phi K^{*+}$ are: $0.01 \pm 0.12 \pm 0.05$, $0.07 \pm 0.15_{-0.03}^{+0.05}$, and $-0.13 \pm 0.29_{-0.11}^{+0.08}$, respectively. These correspond to 90% confidence level limits of $-0.20 < A_{CP}(\phi K^+) < 0.22$, $-0.18 < A_{CP}(\phi K^{*0}(K^+\pi^-)) < 0.33$, and $-0.64 < A_{CP}(\phi K^{*+}) < 0.36$, respectively. The systematic error includes the uncertainties in signal extraction (2%) and detector induced bias (1 – 6%), which has been studied using large samples of inclusive charged kaon and pion tracks, high momentum $D^0 \rightarrow K^-\pi^+$ and $D^+ \rightarrow K^-\pi^+\pi^+$ decays, and B -meson decays to the channels $J/\psi K^{(*)}$, $\bar{D}^0\pi^+$ and $D^{*-}\pi^+$. The systematic errors due to background from $B \rightarrow f_0 K^{(*)}$ and non- K^* background in $B \rightarrow \phi K^*$ channels are also included.

The decay angles of a B -meson, to the two vector mesons ϕ and K^{*0} , as defined in the transversity basis [12], are shown in Fig. 2. The x - y plane is defined by the K^{*0} daughters and the x axis is in the direction of the ϕ -meson. The y axis is perpendicular to the x axis and is on the same side as the kaon from K^{*0} decay. The z axis is perpendicular to the x - y plane according to the right-hand rule. θ_{tr} (ϕ_{tr}) is the polar (azimuthal) angle with respect to the z -axis of the K^+ from ϕ decay in the ϕ rest frame. θ_{K^*} is defined above.

The distribution of decays in the three angles [13], θ_{K^*} , θ_{tr} , and ϕ_{tr} is

$$\begin{aligned} \frac{d^3\Gamma(\phi_{tr}, \cos\theta_{tr}, \cos\theta_{K^*})}{d\phi_{tr}d\cos\theta_{tr}d\cos\theta_{K^*}} = & \frac{9}{32\pi} [|A_\perp|^2 2\cos^2\theta_{tr}\sin^2\theta_{K^*} \\ & + |A_\parallel|^2 2\sin^2\theta_{tr}\sin^2\phi_{tr}\sin^2\theta_{K^*} \\ & + |A_0|^2 4\sin^2\theta_{tr}\cos^2\phi_{tr}\cos^2\theta_{K^*} \\ & + \sqrt{2}\text{Re}(A_\parallel^*A_0)\sin^2\theta_{tr}\sin 2\phi_{tr}\sin 2\theta_{K^*} \\ & - \eta\sqrt{2}\text{Im}(A_0^*A_\perp)\sin 2\theta_{tr}\cos\phi_{tr}\sin 2\theta_{K^*} \\ & - 2\eta\text{Im}(A_\parallel^*A_\perp)\sin 2\theta_{tr}\sin\phi_{tr}\sin^2\theta_{K^*}] , \end{aligned} \quad (1)$$

where A_0 , A_\parallel , and A_\perp are the complex amplitudes of the three helicity states in the transversity basis with the normalization condition $|A_0|^2 + |A_\parallel|^2 + |A_\perp|^2 = 1$, and $\eta \equiv +1$ (-1) for B^0 (\bar{B}^0). A_0 denotes the longitudinal polarization of the $\phi \rightarrow K^+K^-$ system and A_\perp (A_\parallel) is the transverse polarization along the z -axis (y -axis). The value of $|A_\perp|^2$ ($|A_0|^2 + |A_\parallel|^2 \equiv 1 - |A_\perp|^2$) is the CP -odd (CP -even) fraction in the decay $B \rightarrow \phi K^*$ [13]. The imaginary phases of the amplitudes are sensitive to final state interactions (FSI). The presence of FSI results in phases that are not either 0 or $\pm\pi$.

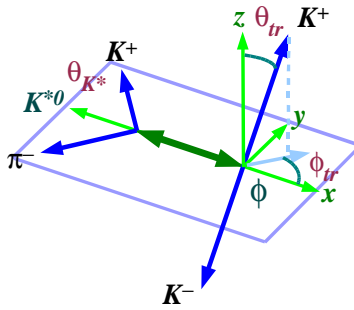


FIG. 2: The definition of decay angles in $B \rightarrow \phi K^{*0}$ decay.

The complex amplitudes are determined by performing an unbinned maximum likelihood fit [14] with $B^0 \rightarrow \phi K^{*0}(K^+\pi^-)$ candidates in the signal window. The combined likelihood

is given by

$$\begin{aligned} \mathcal{L} = & \prod_i^N \epsilon(\theta_{K^*}, \theta_{\text{tr}}, \phi_{\text{tr}}) [f_{\phi K^{*0}} \cdot \Gamma(\theta_{K^*}, \theta_{\text{tr}}, \phi_{\text{tr}}) \\ & + f_{q\bar{q}} \cdot R_{q\bar{q}}(\theta_{K^*}, \theta_{\text{tr}}, \phi_{\text{tr}}) \\ & + f_{KKK^{*0}} \cdot R_{KKK^{*0}}(\theta_{K^*}, \theta_{\text{tr}}, \phi_{\text{tr}})] , \end{aligned} \quad (2)$$

where Γ is the angular distribution function (ADF) given by Eq. 1, and $R_{q\bar{q}}$ and $R_{KKK^{*0}}$ are the ADFs for continuum and $B \rightarrow KKK^{*0}$ background, respectively. The value of η is determined from the charge of the kaon in K^{*0} decay, $R_{q\bar{q}}$ is determined from sideband data and $R_{KKK^{*0}}$ is assumed to be flat. The detection efficiency function (ϵ) is determined by MC. The fractions of ϕK^{*0} ($f_{\phi K^{*0}}$), $q\bar{q}$ ($f_{q\bar{q}}$) and $B \rightarrow KKK^{*0}$ ($f_{KKK^{*0}}$) are parameterized as a function of ΔE and M_{bc} . The value of $\arg(A_0)$ is set to zero and $|A_{\parallel}|^2$ is calculated from the normalization constraint in the fit. Four parameters ($|A_0|^2$, $|A_{\perp}|^2$, $\arg(A_{\parallel})$, and $\arg(A_{\perp})$) are left free to be determined from the fit.

Figure 3 shows projections for each of the three angles together with results from the fit. The amplitudes obtained from the fit are $|A_0|^2 = 0.43 \pm 0.09 \pm 0.04$, $|A_{\perp}|^2 = 0.41 \pm 0.10 \pm 0.04$, $\arg(A_{\parallel}) = -2.57 \pm 0.39 \pm 0.09$, and $\arg(A_{\perp}) = 0.48 \pm 0.32 \pm 0.06$, where the first errors are statistical and the second errors are systematic. The systematic uncertainties include the slow pion detection efficiency (3 – 6%), the background from higher K^* states (6 – 9%), and the $B \rightarrow f_0 K^*$ background (1%). The systematic uncertainty due to the angular resolution is estimated by MC simulation and found to be less than 1%. Uncertainties due to the background PDFs, the signal yields, and the modeling of efficiency function (ϵ) are estimated to be 1 – 3%.

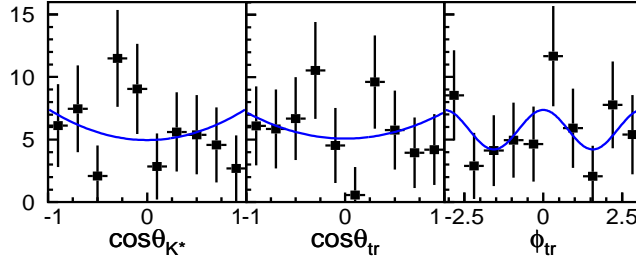


FIG. 3: Projections of the transversity angles with results of the fit superimposed. The points with error bars show the efficiency corrected data after subtraction of continuum and $B \rightarrow K^+ K^- K^*$ background. The $\chi^2/\text{n.d.f.}$ for the projection of $\cos \theta_{K^*}$, $\cos \theta_{\text{tr}}$ and ϕ_{tr} are given by 1.05, 0.90 and 0.46, respectively.

In summary, we measure the branching fractions of four $B \rightarrow \phi K^{(*)}$ decay modes. The value of $\mathcal{B}(B^+ \rightarrow \phi K^+)$ is in good agreement with, and supersedes, previously reported Belle measurements [15, 16]. Our branching fraction results are in agreement with measurements by BABAR [17] and CLEO [18], and the predictions by PQCD [5]. The measured direct CP asymmetries in these modes are consistent with zero. The decay amplitudes for $B^0 \rightarrow \phi K^{*0}$ are determined by fitting the angular distributions in the transversity basis. The longitudinal polarization fraction ($f_L(\phi K^{*0})$) reported by BABAR [19] agrees with our measured value of $|A_0|^2$. The measured value of $|A_{\perp}|^2$ shows that both CP -odd ($|A_{\perp}|^2$) and CP -even ($|A_0|^2 + |A_{\parallel}|^2$) components are present in ϕK^* decays, in contrast to the case of $B \rightarrow J/\psi K^*$,

which is dominantly CP -even [14]. Our data also yield a good fit when the phases of A_{\perp} and A_{\parallel} are constrained to zero and $-\pi$, indicating that our data cannot distinguish the presence of final state interactions.

We wish to thank the KEKB accelerator group for the excellent operation of the KEKB accelerator. We acknowledge support from the Ministry of Education, Culture, Sports, Science, and Technology of Japan and the Japan Society for the Promotion of Science; the Australian Research Council and the Australian Department of Industry, Science and Resources; the National Science Foundation of China under contract No. 10175071; the Department of Science and Technology of India; the BK21 program of the Ministry of Education of Korea and the CHER SRC program of the Korea Science and Engineering Foundation; the Polish State Committee for Scientific Research under contract No. 2P03B 01324; the Ministry of Science and Technology of the Russian Federation; the Ministry of Education, Science and Sport of the Republic of Slovenia; the National Science Council and the Ministry of Education of Taiwan; and the U.S. Department of Energy.

* on leave from Fermi National Accelerator Laboratory, Batavia, Illinois 60510

† on leave from Nova Gorica Polytechnic, Nova Gorica

- [1] N. Cabibbo, Phys. Rev. Lett. **10**, 531 (1963); M. Kobayashi and T. Maskawa, Prog. Theor. Phys. **49**, 652 (1973).
- [2] A. Datta, Phys. Rev. D **66** 071702, (2002).
- [3] R. Fleischer, T. Mannel, Phys. Lett B **511**, 240 (2001).
- [4] H.-Y. Cheng and K.-C Yang, Phys. Rev. D **64** (2001) 074004.
- [5] C.-H. Chen, Y.-Y Keum, and H.-N. Li, Phys. Rev. D **64** (2001) 112002.
- [6] A. Abashian *et al.*, Nucl. Instr. Meth. A **479**, 117 (2002).
- [7] S. Kurokawa, E. Kikutani, Nucl. Instr. Meth. A **499**, 1 (2003).
- [8] We use the S_{\perp} variable as defined in CLEO Collaboration, R. Ammar *et al.*, Phys. Rev. Lett. **71**, 674 (1993), and the thrust angle and modified Fox-Wolfram moments defined in Belle Collaboration, K. Abe *et al.*, Phys. Lett. B **517**, 309 (2001).
- [9] The range corresponds to the range of values for different sub-modes. This convention is used throughout this letter.
- [10] The functional form is $x\sqrt{1-x^2}\exp(\alpha(1-x^2))$, where $x = M_{bc}/E_{\text{beam}}$. ARGUS Collaboration, H. Albrecht *et al.*, Phys. Lett. B **241** (1990) 278; **254** (1991) 288.
- [11] Particle Data Group, K. Hagiwara *et al.*, Phys. Rev. D **66** (2002).
- [12] I. Dunietz, H. Quinn, A. Snyder, W. Toki, and H.J. Lipkin, Phys. Rev. D **43**, 2193 (1991).
- [13] K. Abe, M. Satpathy and H. Yamamoto, hep-ex/0103002 (2001).
- [14] Belle Collaboration, K. Abe *et al.*, Phys. Lett. B **538**, 11 (2002)
- [15] Belle Collaboration, H. Tajima, Int. J. Mod. Phys. A **17**, 2967-2981 (2002).
- [16] Belle Collaboration, A. Garmash *et al.*, Phys. Rev. D **65**, 092005 (2002).
- [17] BABAR Collaboration, B. Aubert *et al.*, Phys. Rev. Lett. **87**, 151801 (2001)
- [18] CLEO Collaboration, R.A. Briere *et al.*, Phys. Rev. Lett. **86**, 3718 (2001).
- [19] BABAR Collaboration, B. Aubert *et al.*, hep-ex/0303020.